Air Quality, Atmosphere & Health (2019) 12:1181–1188
https://doi.org/10.1007/s11869-019-00732-6

Ozone-assisted photocatalytic degradation of gaseous toluene from waste air stream using silica-functionalized graphene oxide/ZnO coated on fiberglass: performance, intermediates, and mechanistic pathways

Ahmad Jonidi Jafari[1,2] · Hossein Arfaeinia[3,4] · Bahman Ramavandi[3,4] · Roshanak Rezaei Kalantary[2] · Ali Esrafily[2]

Received: 1 May 2019 / Accepted: 30 July 2019 / Published online: 4 September 2019

Abstract

The present study focused on the potential of an ozone-assisted photocatalytic process using the catalyst silica-functionalized graphene oxide/ZnO coated on fiberglass (Si-GO/ZnO-FG) in the removal of toluene from waste air stream. Here, a comparative examination was performed in terms of toluene removal efficiency in the photocatalytic process (UV/Si-GO/ZnO-FG) and photocatalytic ozonation (O_3/UV/Si-GO/ZnO-FG). The gaseous intermediates resulting from degradation of toluene by different processes were analyzed using GC-MS. The results of this study indicated that with the addition of ozone to the UV/Si-GO/ZnO-FG process, toluene removal increased significantly from 76.18 to 87.8%. The reason for this incremental efficiency can be explained by the fact that with the addition of ozone, the production rate and the extent of hydroxyl radical ($OH^{\bullet}$) production grow significantly; thereby, more pathways are developed for toluene degradation. The major byproducts in toluene oxidation by photocatalytic and photocatalytic ozonation processes include formic acid, acetic acid, benzyl alcohol, benzaldehyde, *p*-cresol, hydroquinone, and benzoic acid. Given the intermediates and the dominant oxidants detected in the aforementioned process, the possible toluene degradation pathway by the utilized process was suggested.

Keywords Toluene · Waste air · Silica-functionalized graphene oxide · ZnO photocatalyst, ozone

Introduction

Clearing the air from toxic gaseous pollutants is vital for the improvement of the air quality in indoor environments and perseverance of the human health (Mirzaei et al. 2015; Jafari et al. 2018b; Brdarić et al. 2019). In this framework, volatile organic compounds (VOCs) are a group of important pollutants in indoor and ambient air; they are widely emitted into the atmosphere through different industrial processes, vehicle traffic, storage of solvents, and the processing of various raw chemical compounds (Ma et al. 2015; Tabari et al. 2017; Baghani et al. 2018; Arfaeinia et al. 2015). Toluene with the chemical formula of C_6H_5–CH_3 or C_7H_8 is one of the dominant volatile organic compounds (so-called phenyl methane and methyl benzene). It is widely used in industries as solvent for paints including paint thinners, resin, polishers, perfume, plastic, print ink, glue, nail polish, and chemical reactants (Rezaee et al. 2007; Hamid et al. 2019; Ishizaka et al. 2019). Acute exposure to this compound affects the central nervous system causing headache, losing control, convulsion, coma, and death (Larsen and Leira 1988; Goodman et al. 2019). Toluene is also one of the important VOCs in the indoor air of buildings; inherent characteristics including high potential for oxidation and its highly stable structure can be considered a suitable option to assess the photocatalytic properties of semi-conductors (Huang and Li 2011; Rezaei et al. 2013b).

Electronic supplementary material The online version of this article (https://doi.org/10.1007/s11869-019-00732-6) contains supplementary material, which is available to authorized users.

✉ Hossein Arfaeinia
arfaeiniah@yahoo.com

[1] Research Center for Environmental Health Technology, Iran University of Medical Sciences, Tehran, Iran

[2] Department of Environmental Health Engineering, School of Public Health, Iran University of Medical Sciences, Tehran, Iran

[3] Department of Environmental Health Engineering, Faculty of Health and Nutrition, Bushehr University of Medical Sciences, Bushehr, Iran

[4] Systems Environmental Health and Energy Research Center, The Persian Gulf Biomedical Sciences Research Institute, Bushehr University of Medical Sciences, Bushehr, Iran

In spite of advantages such as photosensitivity and suitable energy band for degradation of organic contaminants, zinc oxide (ZnO) has disadvantages such as fast recombination of the photogenerated electron-hole pairs and photoresponding (Hoffmann et al. 1995; Jafari et al. 2017). A solution to overcome these limitations is the use of materials with carbon structure (Woan et al. 2009). Graphene as a carbon compound due to inherent properties including electron interactions with semiconductors inhibits recombination of electric charge in electronic transmission processes, causing enhanced photocatalytic performance (Fu et al. 2008). However, in heterogeneous gas-solid photocatalytic processes which are used for degrading organic wastes, selection of an appropriate support is an important stage as the powdered graphene-zinc oxide (GO/ZnO) composite should be immobilized on a solid-state material before contact with the gaseous molecules of the contaminant. Fiberglass is a solid-state material which has recently been used for stabilizing nano-sized materials exploiting from low cost, lightweight, easy attachment, suitable transparency for natural light, and high stability against ultraviolet radiation as well as excellent mechanical characteristics (Ma et al. 2013; Wong et al. 2014; Liu et al. 2012). In our previous study which was recently published, we successfully immobilized GO/ZnO on fiberglass and used it for photocatalytic removal of benzene from polluted air (Jafari et al. 2018a).

Since photocatalysts may be deactivated in response to the factors such as chemisorption of the intermediates and consequently cause the efficiency of the process to diminish (Boulamanti and Philippopoulos 2008), great attempts have been made to prevent deactivation of catalysts and to enhance the photocatalytic degradation rate. Ozone is a well-known and strong oxidant which has been reported to exert a positive effect on preventing deactivation of photocatalysts and improving their recovery (Zhang and Liu 2004). Nevertheless, the ozone itself has a high oxidizing property causing improved oxidation rate and degradation of organic compounds in the presence of catalysts (Huang et al. 2017).

In the present study, graphene oxide was functionalized with silica and coated on fiberglass. In the next stage, ZnO was coated on the composite just formed in the previous stage through the simple co-precipitation method using chloride as a precursor. The final composite was then called silica-GO/ZnO-incorporated fiberglass composite (Si-GO/ZnO-FG). Next, the synthesized composite was used as a catalyst for photocatalytic removal of toluene from waste air stream in the presence of ozone. Eventually, the products and intermediates resulting from toluene degradation were determined to propose the possible pathways and mechanism of degradation.

Materials and methods

The setup of experiments

A schematic of the reactor and the entire process of experiments is provided in Fig. 1. In this study, a photoreactor made of Pyrex with a volume of 3.84 L (12 × 12 × 16 cm) was used which was completely sealed. For uniform air distribution inside the reactor, an air distributor made of stainless steel was devised in the input part of the reactor, where the distributor's diameter was 6 cm with standard pores of 100–140 mesh. The system consisted of three important parts including the system to produce the input waste air stream, the reactor of photocatalytic reactions, and the equipment to read the contaminant. The system for generating the input waste air stream into the reactor included a blower pump, a dryer, a flow meter, valves, tubes, connections, a syringe pump, a mixing tank, a mixer equipped with an electric fan, a switch key, etc., through which the concentration of input toluene, the level of humidity, and the input air flow rate into the reactor were regulated

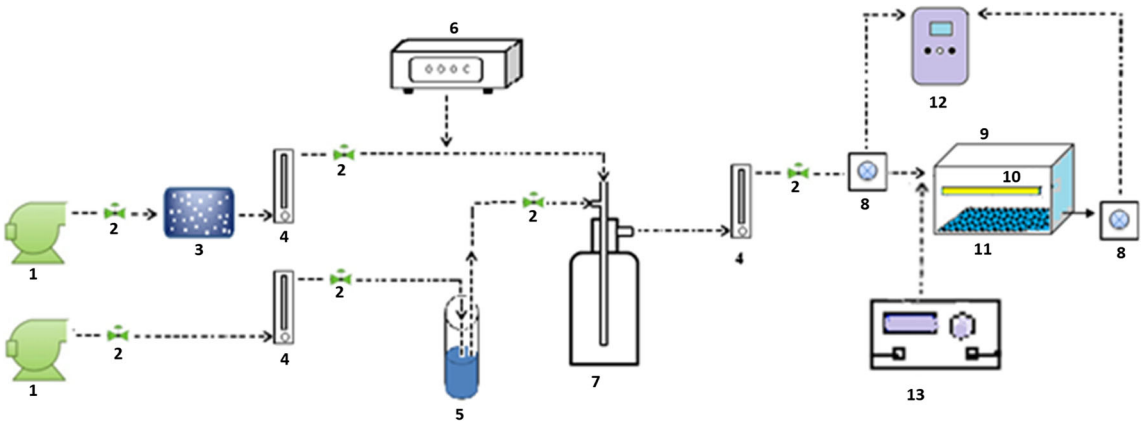

Fig. 1 Schematic flow diagram of the experimental reactor. (1) Air pump, (2) control valve, (3) drier, (4) flow meter, (5) humidifier, (6) syringe pump, (7) mixing chamber, (8) sampling port, (9) reactor, (10) UV lamp, (11) catalyst bed, (12) detection apparatus, and (13) ozone generator

and controlled. An ozone generator (ARDA, model COG-OM, type 1A) with a capacity of 5 g/h was utilized. The ultraviolet (UV) lamp used in this study had a power of 8 W, which was placed vertically in the upper part of the reactor towards the center. The maximum emission and intensity by the lamp were 365 nm and 1.52 mW/cm^2, respectively. The catalyst immobilized on the fiberglass was coated with fiberglass glue 6 cm away from the UV lamp to the reactor walls vertically and the reactor's floor, horizontally.

The photocatalytic ozonation reactor began to operate continuously using the Si-GO/ZnO-FG composite. The method of preparation, synthesis, and properties of this catalyst have been presented in detail in our previous study (Jafari et al. 2018a). The reaction system inside the reactor reaches equilibrium through the following three stages: (1) adjustment of the humidity and concentration of the input toluene into the reactor—the relative humidity and concentration of input toluene were adjusted by adjusting the input gas flow rate and keeping it constant until reaching a specific and constant value and then entering into the reactor. (2) Toluene adsorption equilibrium: the toluene concentration and the input relative humidity before and after the reactor were measured. The point at which the extent of input and output reaches a constant value, dynamic equilibrium, developed between adsorption and desorption, after which UV lamp was turned on. (3) Toluene degradation equilibrium: after turning on the UV lamp and starting the degradation process, the output toluene concentration gradually decreased to get stable, when the degradation reactions reach the equilibrium state. After this stage, the data of removal experiments can be noted down. In each run of experiments and before the experiments with UV radiation, the reactor was placed in a dark condition for 30 min so that the adsorption-desorption equilibrium would develop between the contaminant and catalyst. The input and output toluene concentrations were determined as in interval and noted down. To measure the toluene concentration, the PhoCheck 5000 PID device was employed. The extent of removal efficiency was calculated by the following formula:

$$X = \frac{C_{in} - C_{out}}{C_{in}} \times 100$$

where X represents the extent of removal efficiency (%). C_{in} and C_{out} denote the toluene concentrations in the input and output of the reactor (mg/m^3). To ensure the accuracy of the results, all experiments were replicated for three times.

Determining the byproducts and mechanism of toluene degradation

To determine the byproducts resulting from degradation of toluene by the O_3/UV/Si-GO/ZnO-FG process, an experiment was designed in an optimal state (initial concentration, 100 ppm; relative humidity, 35%; ozone dosage, 0.1 g/h; flow rate, 7.5 L/min; temperature, 25 °C) and then conducted. For this purpose, to collect gaseous products, an impinge containing carbon disulfide (CS_2, HPLC grade) was placed in the reactor out and the output air of the reactor was passed through this bottle for 1 h (off the equilibrium time). In addition, after completion of the mentioned reaction, the utilized catalytic bed was separated from the reactor and washed by carbon disulfide. After this stage, the products obtained from these two processes were mixed together and were injected into gas chromatography (G1530N, Agilent) equipped with mass spectrometry (5973N, MS, Agilent) to determine the byproducts resulting from their degradation. For calculation of the carbon dioxide density (CO_2) in the reactor output, a CO_2 measurement device (Testo 535, Germany) was utilized. This device measures CO_2 concentration within the range of 0–9999 ppm using a dual-channel infrared sensor. Furthermore, to measure the carbon monoxide (CO) concentration, a portable CO detector (CO-mètre CO 50, Kimo Instruments, Inc. Canada) was used. The measurement range of this detector was 0–1000 ppm. In order to measure the density of CO_2 and CO in the reactor output, the device sensor was placed inside a chamber to be exposed to the output air stream leaving the reactor. Once the byproducts were identified, by means of previous studies and relying on the principles of chemistry, the possible pathway of toluene degradation in the photocatalytic ozonation process by the synthesized catalyst (O_3/UV/Si-GO/ZnO-FG) was proposed.

Results and discussion

Catalytic activity test in toluene degradation

The efficiency of different processes of UV (only), O_3 (only), O_3/Si-GO/ZnO-FG, UV/Si-GO/ZnO-FG, and O_3/UV/Si-GO/ZnO-FG in toluene removal (within the range of 50–200 ppm) at the flow rate of 7.5 L/min of the waste air stream was examined. As observed in Fig. 2, toluene removal efficiency decreases with elevation of the initial input concentration through these processes. In heterogeneous catalytic processes, the factors determining the rate-controlling stage include mass transfer and superficial reaction (Hong et al. 2007). Figure 2 shows that the direct degradation of toluene by UV alone or O_3 alone has been negligible. This low removal efficiency is attributable to its aromatic structure, and toluene can hardly be degraded directly by these two processes (Huang and Li 2011). In a catalytic ozonation process with Si-GO/ZnO-FG, the removal efficiency of this contaminant reached around 15–17% in the best case. Toluene removal on the surface of metal oxides is strongly dependent on the capacity of ozone decomposition and formation of active oxygen species (Dhandapani and Oyama 1997; Rezaei et al. 2013a). Therefore, the low toluene removal efficiency by the O_3/Si-GO/ZnO-FG process can be attributed

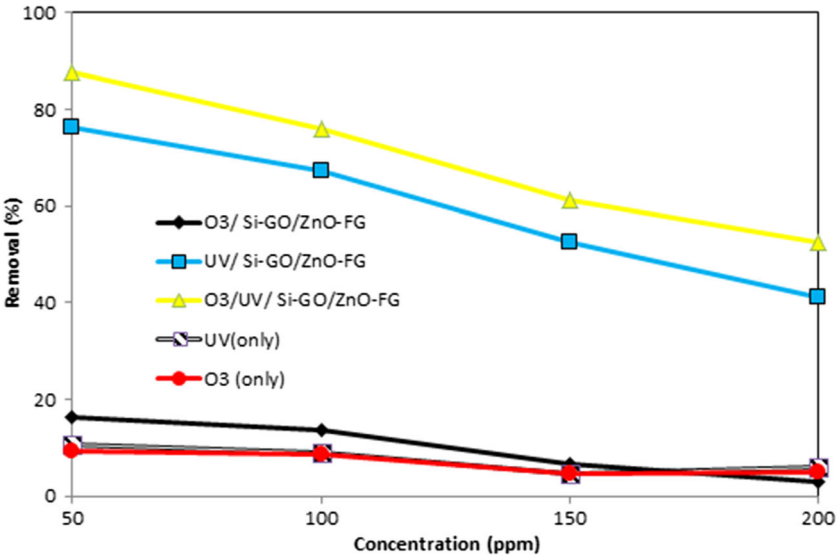

Fig. 2 Toluene removal efficiency under different processes (initial concentration, 50–200 ppm; relative humidity, 35%; ozone dosage, 0.1 g/h; flow rate, 7.5 L/min; temperature, 25 °C)

to low ZnO capacity in ozone decomposition (Huang et al. 2015). In the UV-Si-GO/ZnO-FG process, with elevation of the initial concentration from 50 to 200 ppm, toluene removal efficiency decreased from 76.18 to 41.35%. This high efficiency is mostly due to the photocatalytic activity of the Si-GO/ZnO-FG nano-composite. In the presence of UV, photoexcitation of the catalyst particles causes development of electron-hole pair, and the very high reduction potential of these excited electrons results in development of $OH^{\bullet}$. As it is clear in Eqs. 1–7, $OH^{\bullet}$ and the developed positive holes cause degradation and decomposition of contaminant molecules (Wang et al. 2002; Mehrizadeh et al. 2017).

$$Si{-}GO/ZnO{-}FG + h\upsilon \rightarrow Si{-}GO/ZnO{-}FG(h^{+}{}_{VB}) + Si{-}GO/ZnO{-}FG(e^{-}{}_{CB}) \quad (1)$$

$$O_2 + \mathrm{Si{-}GO/ZnO{-}FG}(e^{-}{}_{CB}) \rightarrow O_2{}^{-*} \quad (2)$$

$$O_2{}^{-*} + H^{+} \rightarrow HO_2{}^{*} \quad (3)$$

$$HO_2{}^{*} + O_2{}^{-*} \rightarrow HO_2{}^{-} + O_2 \quad (4)$$

$$2HO_2{}^{*} \rightarrow O_2 + H_2O_2 \quad (5)$$

$$H_2O_2 + h\upsilon \rightarrow 2OH^{*} \quad (6)$$

$$H_2O_2 + e^{-}{}_{CB} \rightarrow OH^{-} + OH^{*} \quad (7)$$

With high concentration from 50 to 200 ppm, toluene removal efficiency by the UV/O_3/Si-GO/ZnO-FG process has decreased from 87.3 to 52.61%. The diminished removal efficiency with the rise of input toluene concentration can also be attributed to the increased level of the contaminant molecules applied in each column per unit of time. Therefore, the ratio of active sites to the number of toluene molecules diminishes at higher input concentration, causing faster saturation of the catalyst bed (Kwong et al. 2008). Saturation and blockage of active sites of the surface of photocatalysts result in the diminished production of $OH^{\bullet}$ and other active species, thereby reducing the removal efficiency of toluene (Nath et al. 2014).

The removal efficiency grew significantly after the addition of ozone to the UV/Si-GO/ZnO-FG process, where through the photocatalytic ozonation process (UV/O_3/Si-GO/ZnO-FG), toluene removal efficiency was higher than the sum of photocatalytic processes (UV/Si-GO/ZnO-FG) and ozonation alone (O_3 (alone)). Hence, combining these two processes brings about a suitable synergistic effect. Also, after a course of utilization, photocatalysts were deactivated in response to aggregation of the intermediates of degradation of contaminants on their surface and blockage of the active available sites (Lewandowski and Ollis 2003; Piera et al. 2002). Nevertheless, this phenomenon is not observed in the photocatalytic ozonation process, and with the addition of ozone, the durability and reusability of photocatalysts increased. The photocatalytic ozonation process includes several multiple sub-processes including the photocatalytic process (UV/Si-GO/ZnO-FG), ozone photolysis (UV/O_3), catalytic ozonation (O_3/Si-GO/ZnO-FG), and their synergistic processes due to their interactions, occurrence of which altogether causes improved removal efficiency of toluene from the waste air stream.

To corroborate the mineralization of toluene in these processes, the concentration of carbon oxides (COx) was determined in the outlet stream. Figure 3 indicates the concentration of CO or CO_2 produced from toluene degradation via different processes. As can be seen from Fig. 3, no CO and CO_2 were observed during the adsorption, indicating that no toluene was oxidized. As for the UV/Si-GO/ZnO-FG, the outlet concentration of CO and CO_2 reached 78 and 316 ppm, respectively. As for the O_3/UV/Si-GO/ZnO-FG, the outlet concentration of CO and CO_2 reached 96 and 362 ppm, respectively. These results also suggested that the mineralization efficiency grew significantly after the addition of ozone.

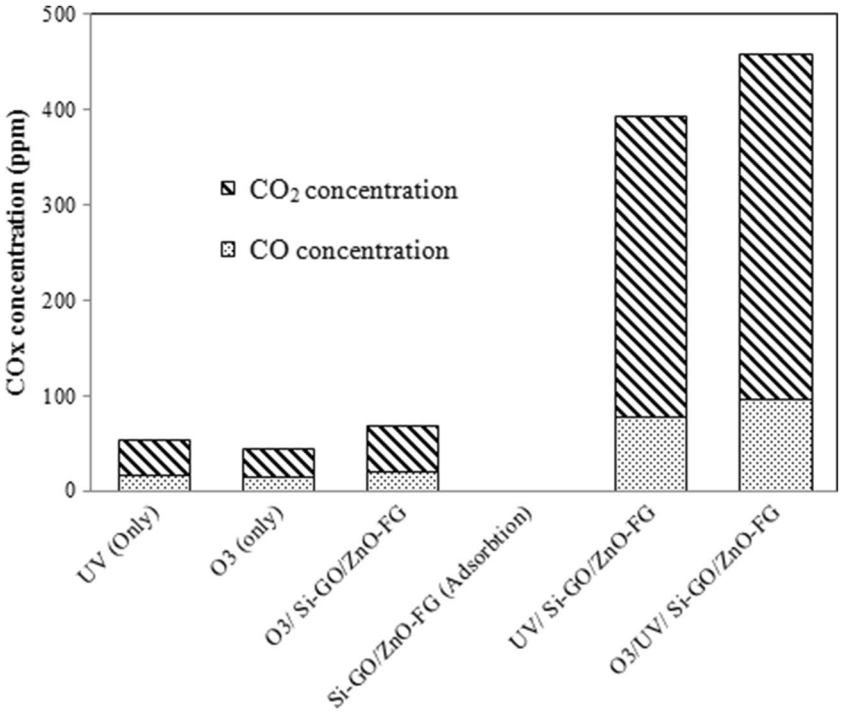

Fig. 3 The concentration of COx under different processes (initial concentration, 100 ppm; relative humidity, 35%; ozone dosage, 0.1 g/h; flow rate, 7.5 L/min; temperature, 25 °C)

The catalyst stability test

The photocatalyst stability and its potential for constant removal of organic contaminants are among very important factors in photocatalytic processes. To evaluate the stability of the synthesized photocatalyst, the experiments were conducted during six runs under the same conditions. After each stage, the catalyst coated with the contaminant was placed

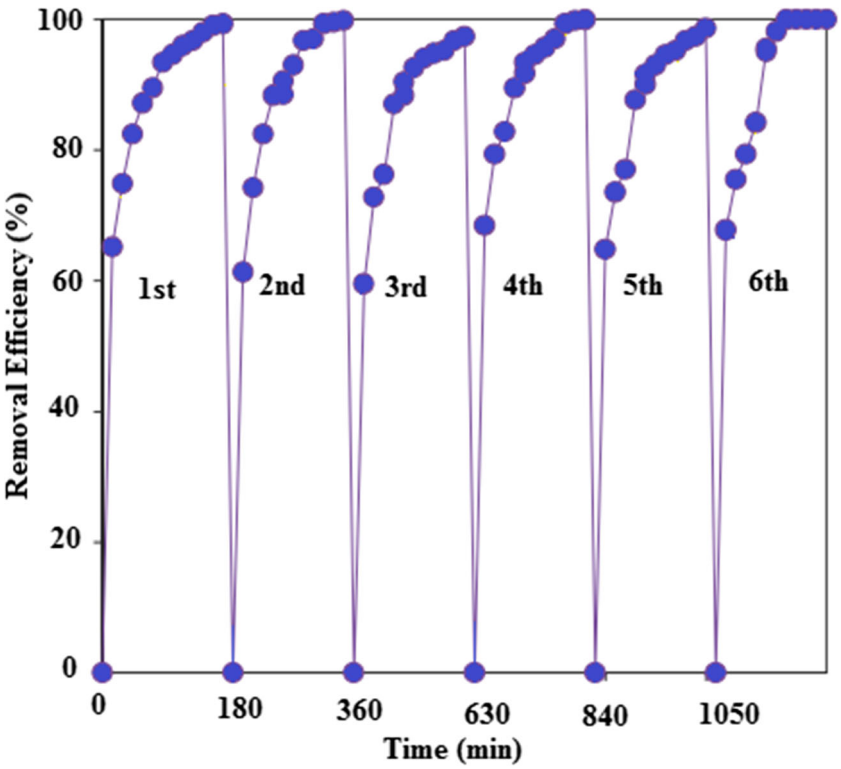

Fig. 4 Reusability profiles of Si-GO/ZnO-FG during repetitive experiments

Table 1 Intermediate species of toluene degradation

Intermediates	Process		
	UV-O_3	UV/Si-GO/ZnO-FG	O_3/UV/Si-GO/ZnO-FG
Formic acid	✓	✓	–
Acetic acid	✓	✓	–
Benzyl alcohol	✓	–	–
Benzaldehyde	✓	✓	✓
p-Cresol	✓	–	–
Hydroquinone	✓	✓	–
Benzoic acid	✓	–	✓

inside sodium hydroxide (NaOH 2 N, as the desorbed agent). Then, toluene photocatalytic degradation experiments from waste air stream by Si-GO/ZnO-FG were performed with five replications, with their results presented in Fig. 4. As can be seen, photocatalytic activity of Si-GO/ZnO-FG still remained high after five runs. This suggests that the catalytic activity of the synthesized photocatalyst can easily be reversed after recovery and slight deactivation occurs for this catalyst.

Degradation of byproducts and mechanism

The mechanism of decomposition of volatile organic compounds through the photocatalytic ozonation process is far more complicated than that of photocatalytic processes. In the photocatalytic process, $OH^{\bullet}$ resulting from oxidation of the absorbed water or absorbed OH^{-1} is known as the initial oxidant, and the photocatalytic degradation reaction is typically controlled by this radical (Yu and Lee 2007). However, with the addition of ozone to the photocatalytic process, the O_3/UV/Si-GO/ZnO-FG process develops, in which several processes including UV/Si-GO/ZnO-FG, UV/O_3, O_3/Si-GO/ZnO-FG, and other processes exist in them due to interaction. Concerning the decomposition of toluene by the O_3/UV/Si-GO/ZnO-FG process, there come two crucial issues: (1) what are the dominant oxidants? (2) How is toluene decomposed by these oxidants?

In the O_3/UV/Si-GO/ZnO-FG process, oxidation of toluene does not occur only on the photocatalyst surface (through UV/Si-GO/ZnO-FG and O_3/Si-GO/ZnO-FG processes), as it rather occurs in the gaseous bulk (through the UV/O_3 process). Therefore, in addition to $OH^{\bullet}$ radical, radical oxygen ($O^{\bullet}$) is also one of the main causes of decomposition. Accordingly, the higher removal efficiency of toluene using

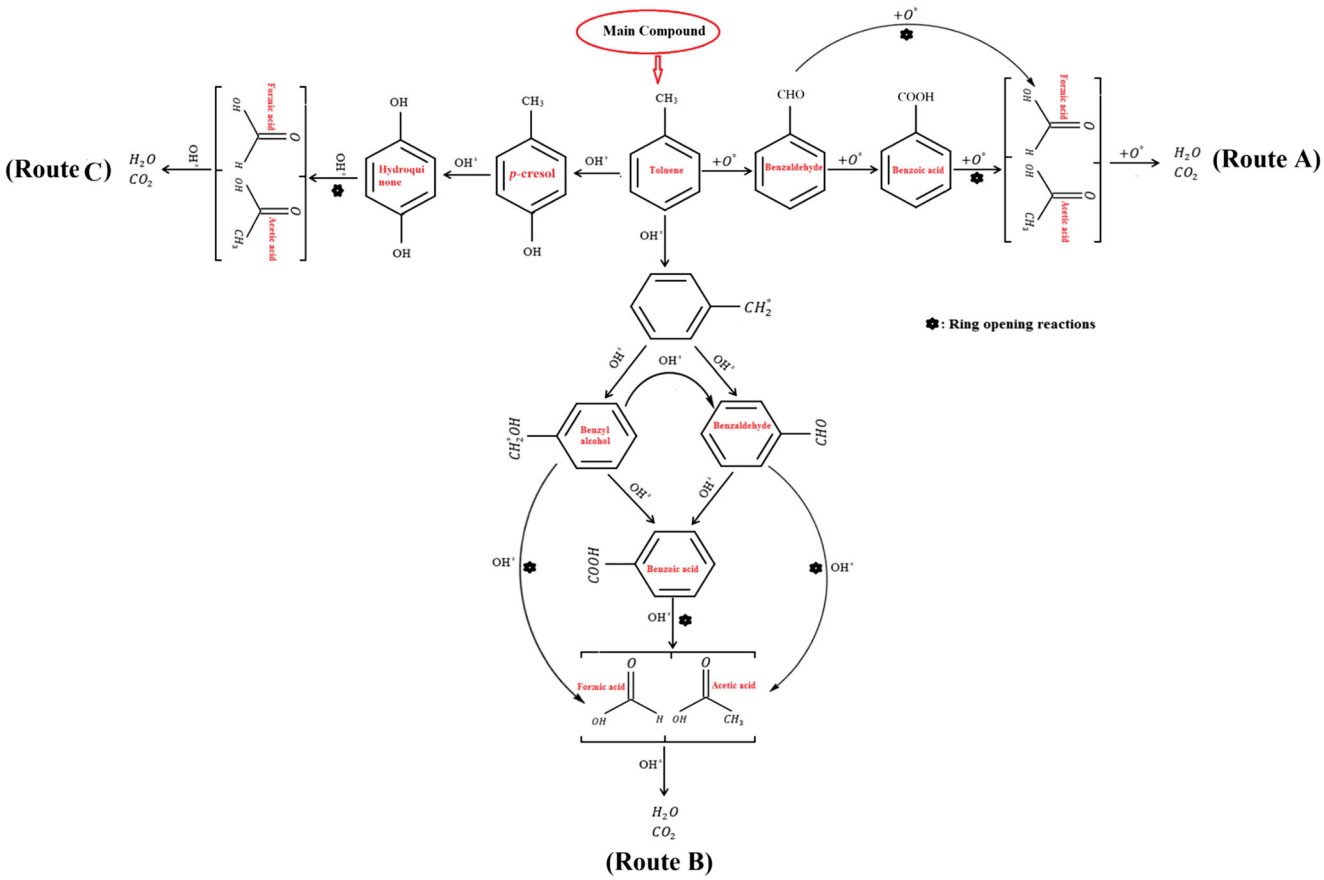

Fig. 5 Possible degradation pathway of toluene molecule under the O_3/UV/Si-GO/ZnO-FG process

the catalytic ozonation process can be attributed to greater production of radicals in this process (Huang and Li 2011).

If the entire input toluene (100 ppm) is completely mineralized and changed into CO and CO_2, 700 ppm carbon oxides should have been formed in the output. However, the sum of CO and CO_2 detected has been less than 450 ppm (see Fig. 3), suggesting the fact that some trace intermediates have also been produced during toluene decomposition by the photocatalytic ozonation process used in this study.

The byproducts resulting from toluene decomposition in the process used here (O_3/UV/Si-GO/ZnO-FG) are shown in Figs. S1–S3 as well as Table 1.

As can be seen, formic acid, acetic acid, benzyl alcohol, benzaldehyde, *p*-cresol, hydroquinone, and benzoic acid are the major byproducts in toluene oxidation by the photocatalytic and photocatalytic ozonation processes. In the UV/O_3 process, formic acid, acetic acid, benzyl alcohol, benzaldehyde, *p*-cresol, hydroquinone, and benzoic acid were observed as the byproducts. In the UV/Si-GO/ZnO-FG process, formic acid, acetic acid, benzaldehyde, and hydroquinone were observed. In comparison with the two previous processes, the type and relative frequency of the intermediates have diminished significantly with the addition of ozone to the process, such that in the O_3/UV/Si-GO/ZnO-FG process, only benzaldehyde and benzoic acid were observed. The reason is high $OH^{\bullet}$ formation rate in the photocatalytic ozonation process (Frankcombe and Smith 2007). In a study conducted by Liu et al. (2019)), nano-diamond-decorated ZnO catalysts were used for photocatalytic degradation of gaseous toluene and they reported similar intermediates. According to literature (Sleiman et al. 2009), the transformation from toluene to CO_2 included three processes: (1) toluene reacted rapidly with $^{\bullet}O_2^-$ species to generate benzaldehyde and benzoic acid gradually, (2) benzoic acid was then confirmed to be oxidized rapidly into oxalic acid that demonstrated the opening of the aromatic ring and decomposed into CO_2 and H_2O finally, and (3) toluene converted into some less reactive/less toxic intermediate with linear structure, including benzene and hydroxylated intermediates (benzaldehyde, benzoic acid, etc.) that were much hardly mineralized to CO_2.

According to the abovementioned oxidants and the byproducts observed by GC-MS, the possible toluene degradation pathway by the photocatalytic ozonation process studied here is shown in Fig. 5. Nevertheless, the proposed mechanism cannot fully explain toluene degradation due to the absence of convincing evidence. Also, due to the existence of many small pathways, the decomposition pathway is highly complex and cannot be proposed with certainty (Huang and Li 2011; Huang et al. 2016).

Conclusion

This is the first research focusing on a combined and Si-GO/ZnO-FG catalyst via UV photolysis to enhance toluene degradation with ozone-assisted oxidation. The results of this study indicated that the addition of ozone to the photocatalytic process in the presence of the mentioned catalyst has effectively caused the elevation of toluene degradation efficiency. It was also observed that the number of gaseous byproducts in the O_3/UV/Si-GO/ZnO-FG process has been much lower than that of UV/Si-GO/ZnO-FG. The enhancement effect is mostly attributed to the oxidants that have been formed alongside OH as well as more pathways and high OH production rate. In the photocatalytic ozonation process, $OH^{\bullet}$ and $O^{\bullet}$ have been among the main causes of toluene oxidation. According to the observed byproducts and relying on the principles of chemistry, the possible pathway was proposed for toluene decomposition via the photocatalytic ozonation process in the presence of Si-GO/ZnO-FG.

Acknowledgments The authors gratefully acknowledge the Iran Medical Sciences for technically supporting this research.

Funding information This study received financial support from the Iran Medical Sciences (Grant No. 95-03-27-29472).

References

Arfaeinia H, Moradi M, Sharafi K, Mahdi Esfahan N, Dobaradaran S (2015) Evaluation of public health impacts related to urban air pollution in Shiraz and Bushehr, Iran. Int J Pharm Technol 7:9811–9824

Baghani AN, Rostami R, Arfaeinia H, Hazrati S, Fazlzadeh M, Delikhoon M (2018) BTEX in indoor air of beauty salons: risk assessment, levels and factors influencing their concentrations. Ecotox Environ Safe 159:102–108. https://doi.org/10.1016/j.ecoenv.2018.04.044

Boulamanti AK, Philippopoulos CJ (2008) Photocatalytic degradation of methyl tert-butyl ether in the gas-phase: a kinetic study. J Hazard Mater 160:83–87. https://doi.org/10.1016/j.jhazmat.2008.02.087

Brdarić D, Kovač-Andrić E, Šapina M, Kramarić K, Lutz N, Perković T, Egorov A (2019) Indoor air pollution with benzene, formaldehyde, and nitrogen dioxide in schools in Osijek, Croatia. Air Qual Atmos Health 1:1–6. https://doi.org/10.1007/s11869-019-00715-7

Dhandapani B, Oyama ST (1997) Gas phase ozone decomposition catalysts. Appl Catal B Environ 11:129–166. https://doi.org/10.1016/S0926-3373(96)00044-6

Frankcombe TJ, Smith SC (2007) OH-initiated oxidation of toluene. 1. Quantum chemistry investigation of the reaction path. J Phys Chem A 111:3686–3690. https://doi.org/10.1021/jp067112i

Fu H, Xu T, Zhu S, Zhu Y (2008) Photocorrosion inhibition and enhancement of photocatalytic activity for ZnO via hybridization with C60. Environ Sci Technol 42:8064–8069. https://doi.org/10.1021/es801484x

Goodman NB, Wheeler AJ, Paevere PJ, Agosti G, Nematollahi N, Steinemann A (2019) Emissions from dryer vents during use of fragranced and fragrance-free laundry products. Air Qual Atmos Health 12:289–295. https://doi.org/10.1007/s11869-018-0643-8

Hamid HH, Latif MT, Nadzir MS, Uning R, Khan MF, Kannan N (2019) Ambient BTEX levels over urban, suburban and rural areas in

Malaysia. Air Qual Atmos Health 12:341–351. https://doi.org/10.1007/s11869-019-00664-1

Hoffmann MR, Martin ST, Choi W, Bahnemann DW (1995) Environmental applications of semiconductor photocatalysis. Chem Rev 95:69–96. https://doi.org/10.1021/cr00033a004

Hong QI, SUN DZ, CHI GQ (2007) Formaldehyde degradation by UV/TiO2/O3 process using continuous flow mode. J Environ Sci 19:1136–1140. https://doi.org/10.1016/S1001-0742(07)60185-5

Huang H, Li W (2011) Destruction of toluene by ozone-enhanced photocatalysis: performance and mechanism. Appl Catal B Environ 102:449–453. https://doi.org/10.1016/j.apcatb.2010.12.025

Huang H, Huang W, Xu Y, Ye X, Wu M, Shao Q, Ou G, Peng Z, Shi J, Chen J, Feng Q (2015) Catalytic oxidation of gaseous benzene with ozone over zeolite-supported metal oxide nanoparticles at room temperature. Catal Today 258:627–633. https://doi.org/10.1016/j.cattod.2015.01.006

Huang H, Huang H, Zhan Y, Liu G, Wang X, Lu H, Xiao L, Feng Q, Leung DY (2016) Efficient degradation of gaseous benzene by VUV photolysis combined with ozone-assisted catalytic oxidation: performance and mechanism. Appl Catal B Environ 186:62–68. https://doi.org/10.1016/j.apcatb.2015.12.055

Huang H, Lu H, Zhan Y, Liu G, Feng Q, Huang H, Wu M, Ye X (2017) VUV photo-oxidation of gaseous benzene combined with ozone-assisted catalytic oxidation: effect on transition metal catalyst. Appl Surf Sci 391:662–667. https://doi.org/10.1016/j.apsusc.2016.07.040

Ishizaka TD, Kawashima A, Hishida N, Hamada N (2019) Measurement of total volatile organic compound (TVOC) in indoor air using passive solvent extraction method. Air Qual Atmos Health 12:173–187. https://doi.org/10.1007/s11869-018-0639-4

Jafari AJ, Kermani M, Kalantary RR, Arfaeinia H (2017) Photocatalytic abatement of o-xylene using adsorption enhanced ZnO/GAC catalyst in a continuous flow reactor: catalytic potential. Glob Nest J 19:479–488

Jafari AJ, Kalantary RR, Esrafili A, Arfaeinia H (2018a) Synthesis of silica-functionalized graphene oxide/ZnO coated on fiberglass and its application in photocatalytic removal of gaseous benzene. Process Saf Environ 116:377–387. https://doi.org/10.1016/j.psep.2018.03.015

Jafari AJ, Kermani M, Kalantary RR, Arfaeinia H (2018b) The effect of traffic on levels, distribution and chemical partitioning of harmful metals in the street dust and surface soil from urban areas of Tehran, Iran. Environ Earth Sci 772:38. https://doi.org/10.1007/s12665-018-7226-8

Kwong CW, Chao CY, Hui KS, Wan M (2008) Catalytic ozonation of toluene using zeolite and MCM-41 materials. Environ Sci Technol 42:8504–8509. https://doi.org/10.1021/es801087f

Larsen F, Leira HL (1988) Organic brain syndrome and long-term exposure to toluene: a clinical, psychiatric study of vocationally active printing workers. J Occup Med 30:875–878. https://doi.org/10.1097/00043764-198811000-00014

Lewandowski M, Ollis DF (2003) Extension of a two-site transient kinetic model of TiO2 deactivation during photocatalytic oxidation of aromatics: concentration variations and catalyst regeneration studies. Appl Catal B Environ 45:223–238. https://doi.org/10.1016/S0926-3373(03)00165-6

Liu Z, Fang P, Wang S, Gao Y, Chen F, Zheng F, Liu Y, Dai Y (2012) Photocatalytic degradation of gaseous benzene with CdS-sensitized TiO2 film coated on fiberglass cloth. J Mol Catal A Chem 363:159–165. https://doi.org/10.1016/j.molcata.2012.06.004

Liu J, Wang P, Qu W, Li H, Shi L, Zhang D (2019) Nanodiamond-decorated ZnO catalysts with enhanced photocorrosion-resistance for photocatalytic degradation of gaseous toluene. Appl Catal B Environ 19:117880. https://doi.org/10.1016/j.apcatb.2019.117880

Ma PC, Liu JW, Gao SL, Mäder E (2013) Development of functional glass fibres with nanocomposite coating: a comparative study. Compos A Appl Sci Manuf 44:16–22. https://doi.org/10.1016/j.compositesa.2012.08.027

Ma Y, Li Y, Mao M, Hou J, Zeng M, Zhao X (2015) Synergetic effect between photocatalysis on TiO2 and solar light-driven thermocatalysis on MnOx for benzene purification on MnOx/TiO2 nanocomposites. J Mater Chem A 3(10):5509–5516. https://doi.org/10.1039/C5TA00126A

Mehrizadeh H, Niaei A, Tseng HH, Salari D, Khataee A (2017) Synthesis of ZnFe2O4 nanoparticles for photocatalytic removal of toluene from gas phase in the annular reactor. J Photochem Photobiol A 332:188–195. https://doi.org/10.1016/j.jphotochem.2016.08.028

Mirzaei N, Arfaeinia H, Moradi M, Mohammadi Moghadam F, Velayati A, Sharafi K (2015) The statistical analysis of seasonal and time variations on trend of important air pollutants (SO2, O3, NOx, CO, PM10)-in western Iran: a case study. Int J Pharm Technol 7:9610–9622

Nath RK, Zain MF, Kadhum AA, Kaish AB (2014) An investigation of LiNbO3 photocatalyst coating on concrete surface for improving indoor air quality. Constr Build Mater 54:348–353. https://doi.org/10.1016/j.conbuildmat.2013.12.072

Piera E, Ayllón JA, Doménech X, Peral J (2002) TiO2 deactivation during gas-phase photocatalytic oxidation of ethanol. Catal Today 76:259–270. https://doi.org/10.1016/S0920-5861(02)00224-9

Rezaee A, Khavanin A, Saraf Mamoori R, Hajizadeh E (2007) Elimination of toluene by application of ultraviolet irradiation on TiO2 nano particles photocatalyst. J Mil Med 9:217–222

Rezaei E, Soltan J, Chen N (2013a) Catalytic oxidation of toluene by ozone over alumina supported manganese oxides: effect of catalyst loading. Appl Catal B Environ 136:239–247. https://doi.org/10.1016/j.apcatb.2013.01.061

Rezaei E, Soltan J, Chen N, Lin J (2013b) Effect of noble metals on activity of MnOx/γ-alumina catalyst in catalytic ozonation of toluene. Chem Eng J 214:219–228. https://doi.org/10.1016/j.cej.2012.10.044

Sleiman M, Conchon P, Ferronato C, Chovelon JM (2009) Photocatalytic oxidation of toluene at indoor air levels (ppbv): towards a better assessment of conversion, reaction intermediates and mineralization. Appl Catal B Environ 86:159–165. https://doi.org/10.1016/j.apcatb.2008.08.003

Tabari T, Singh D, Jamali SS (2017) Enhanced photocatalytic activity of mesoporous ZnFe2O4 nanoparticles towards gaseous benzene under visible light irradiation. J Environ Chem Eng 5:931–939. https://doi.org/10.1016/j.jece.2017.01.016

Wang KH, Jehng JM, Hsieh YH, Chang CY (2002) The reaction pathway for the heterogeneous photocatalysis of trichloroethylene in gas phase. J Hazard Mater 90:63–75. https://doi.org/10.1016/S0304-3894(01)00331-4

Woan K, Pyrgiotakis G, Sigmund W (2009) Photocatalytic carbon-nanotube–TiO2 composites. Adv Mater 21:2233–2239. https://doi.org/10.1002/adma.200802738

Wong TT, Lau KT, Tam WY, Leng J, Etches JA (2014) UV resistibility of a nano-ZnO/glass fibre reinforced epoxy composite. Mater Des (1980-2015) 56:254–257. https://doi.org/10.1016/j.matdes.2013.11.014

Yu KP, Lee GW (2007) Decomposition of gas-phase toluene by the combination of ozone and photocatalytic oxidation process (TiO2/UV, TiO2/UV/O3, and UV/O3). Appl Catal B Environ 75:29–38. https://doi.org/10.1016/j.apcatb.2007.03.006

Zhang P, Liu J (2004) Photocatalytic degradation of trace hexane in the gas phase with and without ozone addition: kinetic study. J Photochem Photobiol A 167:87–94. https://doi.org/10.1016/j.jphotochem.2004.05.015